Journal of Applied Electrochemistry (2006) 36:1051–1056
DOI 10.1007/s10800-006-9158-3

Optical, electrical and discharge profiles for (PVC + $NaIO_4$) polymer electrolytes

CH. V. SUBBA REDDY, QUAN-YAO ZHU, LI-QIANG MAI and WEN CHEN*
School of Materials Science and Engineering, Wuhan University of Technology, Wuhan, 430070, China
*(*author for correspondence, tel.: +86-27-87651107, fax: +86-27-87864580, e-mail: chenw@mail.whut.edu.cn)*

Received 21 December 2005; accepted in revised form 9 May 2006

Key words: absorption edge, direct energy gap, discharge profiles, indirect energy gap, ionic conductivity, IR studies, optical absorption spectra, XRD

Abstract

A sodium ion conducting polymer electrolyte based on poly (vinyl chloride) (PVC) complexed with $NaIO_4$ was prepared using a solution-cast technique. Optical properties such as direct and indirect optical energy gap, and optical absorption edge were investigated in pure and doped PVC films from their optical absorption spectra in the 200–600 nm wavelength region. The direct optical energy gap for pure PVC lies at 3.14 eV while it ranges from 2.60 to 3.45 eV for different composition doped films. Similar behavior was observed for the indirect optical energy gap and absorption edge. It was found that the energy gaps and band edge values shifted to higher energies on doping with $NaIO_4$ up to a dopant concentration of 10 wt%. Measurements of ionic conductivity and transference number were made to investigate the order of conductivity and charge transport in this polymer electrolyte. Transference number values show that the charge transport in this polymer electrolyte is predominantly due to ions ($t_{ion} = 0.93$). The conductivity increases with increase in concentration of the salt and with temperature. Using this electrolyte, cells were fabricated and their discharge profiles were studied under constant load. Miscibility studies were performed using X-ray diffraction (XRD) and Fourier Transform Infrared analysis (FT-IR) measurements.

1. Introduction

In recent years, the electrical and optical properties of polymers have attracted much attention in view of their applications in optical devices with remarkable reflection, antireflection, interference and polarization properties [1–5]. The optical properties of polymers can be suitably modified by the addition of dopants depending on their reactivity with the host matrix. As $NaIO_4$ is a fast-ion conducting salt in a number of crystalline and amorphous materials, its incorporation in a polymeric system may be expected to enhance the electrical and optical performance [6].

Polymer electrolytes are currently of interest owing to their advantageous mechanical properties, ease of fabrication of thin films of desired sizes and suitability for electrode–electrolyte contacts in different electrochemical devices. Interest in this field followed studies of materials based on alkali metal salts complexed with polyethylene oxide (PEO) reported by Wright et al. [7, 8] and Armand et al. [9, 10]. PEO/metal–salt complexes exhibit high ionic conductivities at (or) near ambient temperature and thus are attractive candidates for electrochemical applications. The poor mechanical strength of PEO electrolytes in the high conduction region is, however, a severe drawback.

Poly (vinyl chloride) (PVC) is a commercially available, inexpensive polymer and is compatible with many plasticizers such as dibutyl phthalate (DBP), dioctyl adipate (DOA), dioctyl phthalate (DOP), poly carbonate (PC) and ethylene carbonate (EC). The resulting plasticized PVC has good mechanical strength and is widely used in the form of films, sheets, and moldings for plastic leather and curtains, lead–wire coating, flooring, wallboard, etc.

In the present paper, we report solid polymer electrolyte films of PVC and (PVC + $NaIO_4$) systems. Several experimental techniques, such as optical, electrical, XRD, IR and transport number measurements, were performed to characterize these polymer electrolytes. Based on these electrolytes, electrochemical cells were fabricated with the configuration anode/polymer electrolyte/cathode. The discharge characteristics of the cell were studied for a load of 100 kΩ.

2. Experimental

Films of (thickness ≈100–200 μm) PVC, (PVC + $NaIO_4$) (90:10), (80:20) and (70:30) were prepared by the solution-cast technique using tetrahydrofuran (THF) as solvent. The mixture of these

solutions was stirred for 12 h, cast onto polypropylene dishes and evaporated slowly at room temperature. The final product was vacuum dried thoroughly at 10^{-3} mbar.

The optical absorption studies of PVC and (PVC + $NaIO_4$) systems were performed by means of a JASCO spectrophotometer, model V-570 in the wavelength range 310–450 nm. The XRD patterns of the films were made with a HZG4/B-PC X-ray diffractrometer with CoKα radiation and graphite monochrometer. The IR spectra were recorded using a 60-SXB FTIR spectrophotometer in the range 400–4000 cm^{-1}. The conductivity was studied as a function of temperature using a conductivity cell designed in house. The total ionic transport number (t_{ion}) was measured using Wagner's polarization technique [11]. In this technique the freshly prepared polymer electrolyte films were polarized in the configuration C/polymer electrolyte/C under a dc bias (step potential 1.5 V). The resulting current was monitored as a function of time. After polarizing the electrolyte, the transport number, t_{ion}, was calculated from the initial current, I_i, and final residual current, I_f, using the formulae

$$t_{ion} = (I_i - I_f)/I_i, \quad (1)$$

$$t_{ele} = 1 - t_{ion} \quad (2)$$

Electrochemical cells were fabricated with a configuration Na/(PVC + $NaIO_4$)/(I_2 + C). Details regarding the electrochemical cell were given elsewhere [12]. The discharge characteristics of these cells were monitored for a constant load of 100 kΩ.

3. Results and discussion

3.1. *XRD measurements*

Figure 1 shows the XRD patterns of pure $NaIO_4$ and $NaIO_4$ doped PVC polymer electrolyte films. The patterns of complexed PVC indicate low crystallinity. By contrast, $NaIO_4$ is found to be crystalline. No peaks corresponding to pure $NaIO_4$ are observed in complexed PVC. This indicates the absence of excess salt in the complexed polymer films.

3.2. *FTIR studies*

IR spectra of $NaIO_4$ + PVC electrolytes of different compositions were shown in Figure 2(a–c). The vibrational peaks of complexed polymer electrolytes were shifted towards higher wavenumbers with the increased $NaIO_4$ concentration. Figure 2(d) shows IR spectra of $NaIO_4$ salt which shows the peaks at wavenumbers 3415, 3227, 1616 and 843 cm^{-1}. The absence of vibrational peaks of pure $NaIO_4$ salt in the complexed systems and also peak shifts with $NaIO_4$ concentration indicates the miscibility of the salt in the prepared electrolyte systems. In addition to the PVC and $NaIO_4$ salt vibrational peaks, some other peaks were observed at the frequencies 1976 and 1483 cm^{-1} and these peaks were assigned to CH_3 asymmetric stretching and bending vibrations of PVC. The appearance of new peaks along with changes in existing peaks in IR spectra directly indicates the complexation of PVC with $NaIO_4$.

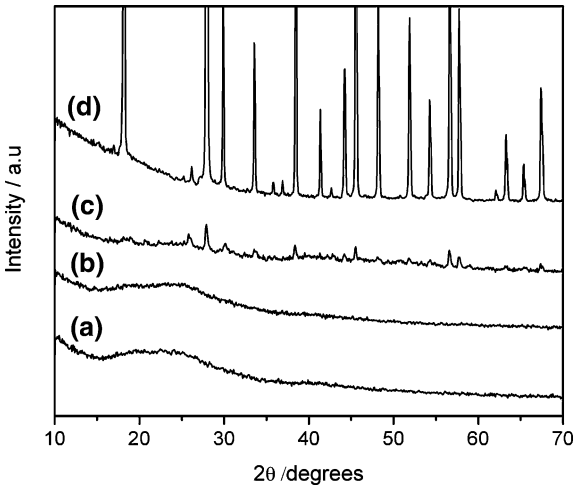

Fig. 1. XRD patterns of $NaIO_4$ complexed PVC: (a) (PVC + $NaIO_4$) (90:10), (b) (PVC + $NaIO_4$) (80:20), (c) (PVC + $NaIO_4$) (70:30), and (d) Pure $NaIO_4$.

3.3. *Optical studies*

Optical absorption studies on pure PVC and $NaIO_4$ doped PVC films were carried out to determine the optical constants such as optical band gap (E_g) and the position of the fundamental band edge. The absorption coefficient was determined from the spectra using the formula

$$\alpha = A/d \quad (3)$$

where A is absorbance and d is film thickness.

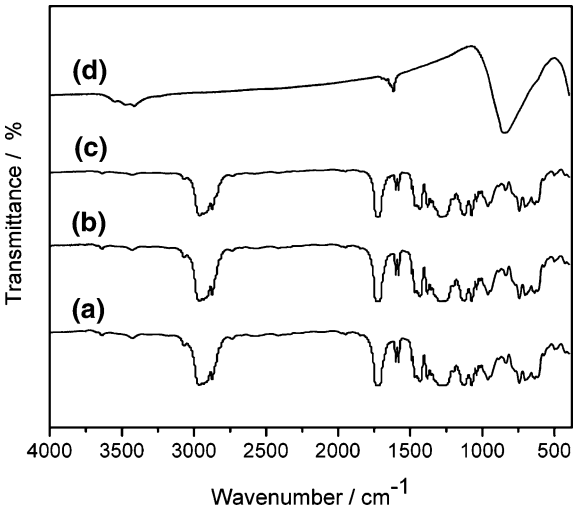

Fig. 2. IR spectra of $NaIO_4$ complexed PVC: (a) (PVC + $NaIO_4$) (90:10), (b) (PVC + $NaIO_4$) (80:20), (c) (PVC + $NaIO_4$) (70:30), and (d) Pure $NaIO_4$.

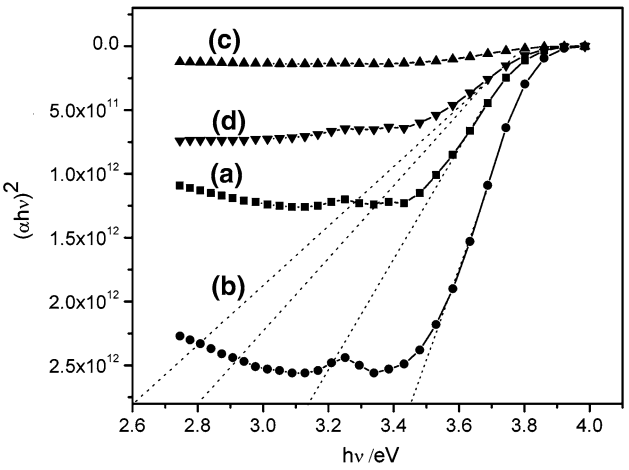

Fig. 3. $(\alpha h\nu)^2$ vs. $h\nu$(photon energy) of (a) pure PVC, (b) (PVC + $NaIO_4$) (90:10), (c) (PVC + $NaIO_4$) (80:20), (d) (PVC + $NaIO_4$) (70:30).

When the direct gap exists, the absorption coefficient has the following dependence on the energy of the incident photon [13, 14].

$$\alpha h\nu = C(h\nu - E_g)^{1/2} \quad (4)$$

where E_g is the band gap, C a constant dependent on spectrum structure, ν the frequency of the incident light and h Plank's constant. Thus, a plot of $(\alpha h\nu)^2$ vs. photon energy $h\nu$ as shown in Figure 3 should be linear. The intercept on the energy on extrapolating the linear portion of the curves to zero absorption value may be interpreted as the value of the band gap. For pure film the direct band gap lies at 3.14 eV, while for doped films the values are given in Table 1.

For indirect transitions, which require photon assistance, the absorption coefficient has the following dependence on the photon energy [13, 14].

$$\alpha h\nu = A[h\nu - E_g + E_p]^2 + B[h\nu - E_g - E_p]^2 \quad (5)$$

where E_p is the energy of the photon associated with the transition, and A and B are constants depending on the band structure. The indirect band gaps were obtained from the plots of $(\alpha h\nu)^{1/2}$ vs. photon energy as shown in Figure 4 and are given in the Table 1.

The position of the absorption edge values were calculated by extrapolating the linear portions of the α vs. h ν plot as shown in Figure 5 to zero absorption value. For pure film, the absorption edge lay at 3.40 eV and for 10, 20 and 30% wt. ratios of $NaIO_4$ doped films values are given in Table 1.

It is clear from Table 1 that the band edge, direct band gap and indirect band gap showed an increase on doping with $NaIO_4$ salt up to a doping concentration of 10 wt%. Similar behaviour can also be seen in the activation energies obtained from the ionic conductivity data as shown in Table 1. This type of behaviour has also been observed in many polymer films [15–19]. The magnitude of the activation energies obtained from conductivity data is small in comparison with optical band gap energies. This is due to the fact that their nature is different. While the activation energy corresponds to the energy required for conduction from one site to another, the optical band gap corresponds to inter band transition [20].

3.4. *Conductivity studies*

The ionic conductivity were determined from ac impedance analysis using the cell with blocking electrodes as described in the experimental section. A typical impedance plot of (PVC + $NaIO_4$) (90:10) at ambient temperature is shown in Figure 6. The bulk resistance was measured from the high frequency intercept on the real axis. The conductivity of the polymer electrolyte was calculated from the measured resistance and the area and thickness of the polymer film.

The variation of the logarithm of ionic conductivity with inverse absolute temperature for the polymer films is presented in Figure 7. The regression values close to unity suggest that the temperature dependent ionic conductivity for all the $NaIO_4$ complexed films obeys the Arrhenius rule. From Figure 7, the conductivity plots of all polymer films show no abrupt jump with temperature, indicating that these electrolytes exhibit a completely amorphous structure [21]. The increase in conductivity with temperature can be linked to the decrease in viscosity and, hence, increased chain flexibility [22]. Since the conductivity–temperature data follow Arrhenius behaviour, the nature of cation transport is quite similar to that in ionic crystals, where ions jump into neighbouring vacant sites [23]. The activation energy (E_a) was calculated from the log(σ) vs. $1000/T$ plots and is noted in the Table 1.

Table 1. Absorption edge, optical band gap, activation energy and transference numbers of (PVC + $NaIO_4$) polymer electrolyte system (PES)

PES/wt% (PVC + $NaIO_4$)	Absorption edge/eV	Band gap/eV		Activation energy/eV	Transference numbers	
		Direct	Indirect		t_{ion}	t_{ele}
100	3.10	3.14	3.40	–	–	–
90:10	3.40	3.45	3.60	0.43	0.93	0.07
80:20	2.70	2.60	3.00	0.32	0.87	0.13
70:30	2.98	2.80	3.30	0.25	0.90	0.10

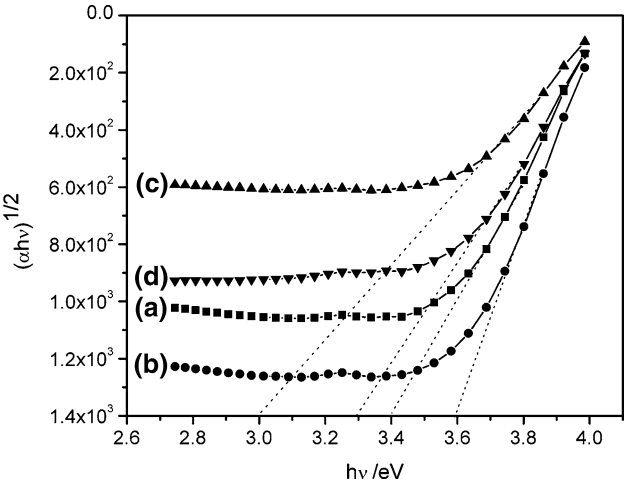

Fig. 4. $(\alpha h\nu)^{1/2}$ vs. $h\nu$(photon energy) of (a) pure PVC, (b) (PVC + $NaIO_4$) (90:10), (c) (PVC + $NaIO_4$) (80:20), (d) (PVC + $NaIO_4$) (70:30).

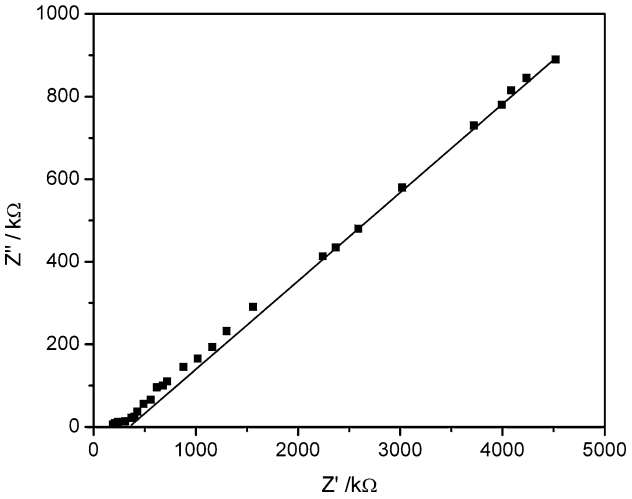

Fig. 6. Impedance plot of (PVC + $NaIO_4$) (90:10) polymer electrolyte at ambient temperature.

3.5. *Transference numbers*

The transference numbers corresponding to ionic (t_{ion}) and electronic (t_{ele}) transport were evaluated in the (PVC + $NaIO_4$) electrolyte system using Wagner's polarization technique. In this technique, the dc current is monitored as a function of time on the application of fixed dc voltage (1.5 V) across a C/(PVC + $NaIO_4$)/C cell. The plot for (PVC + $NaIO_4$) of (90:10) is given in Figure 8. The transference numbers (t_{ion} and t_{ele}) were calculated from the polarization current vs. time plot using equations given in (1) and (2). The resulting data are given in Table 1. For all the compositions of the (PVC + $NaIO_4$) electrolyte system, the values of ionic transference numbers (t_{ion}) are in the range 0.87–0.93 (see Table 1). This suggests that the charge transport in these polymer electrolyte films is predominantly due to ions; only a negligible contribution comes from the electrons.

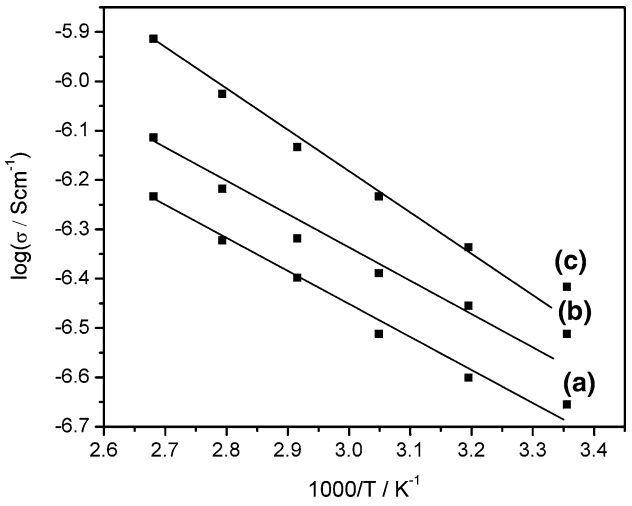

Fig. 7. Plots of log of AC conductivity vs. $1000/T$ for (a) (PVC + $NaIO_4$) (90:10), (b) (PVC + $NaIO_4$) (80:20), (c) (PVC + $NaIO_4$) (70:30).

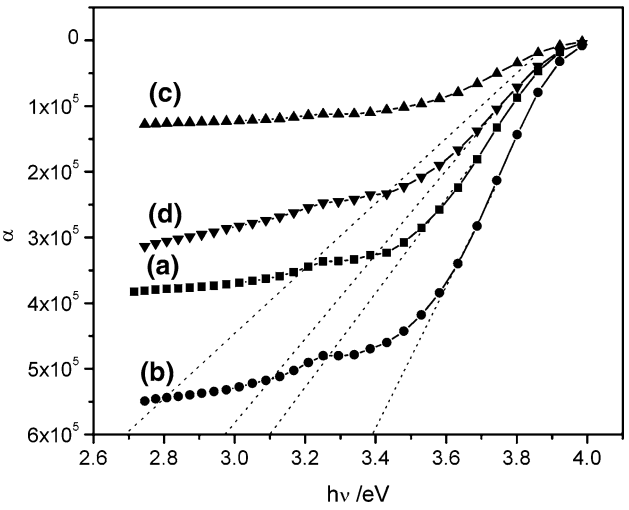

Fig. 5. α vs. $h\nu$(photon energy) of (a) pure PVC, (b) (PVC + $NaIO_4$) (90:10), (c) (PVC + $NaIO_4$) (80:20), (d) (PVC + $NaIO_4$) (70:30).

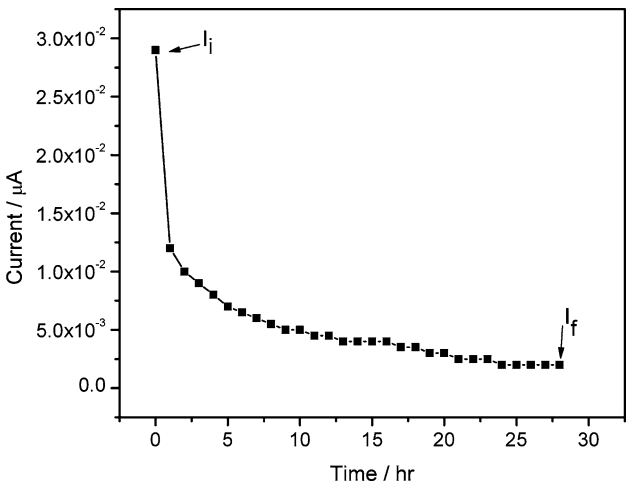

Fig. 8. Plot of current vs. time for (PVC + $NaIO_4$) (90:10) polymer electrolyte.

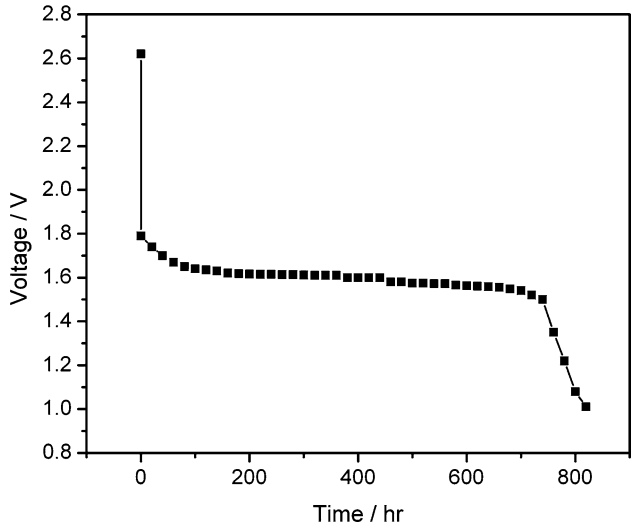

Fig. 9. Discharge characteristics of solid-state electrochemical cell in the configuration Na/(PVC + $NaIO_4$) (90:10)/(I_2 + C).

3.6. *Discharge profiles*

Using (PVC + $NaIO_4$) polymer electrolyte films, solid-state electrochemical cells were fabricated with the configuration Na (anode)/(PVC + $NaIO_4$)/(I_2 + C) (cathode). Sodium metal was used as the negative electrode, and a mix of iodine (I_2) and graphite (C) in the ratio of 5:5 as the positive electrode.

The discharge characteristics of the cells Na/(PVC + $NaIO_4$) (90:10)/(I_2 + C) at ambient temperature for a constant load of 100 kΩ are presented in Figure 9. The initial sharp decrease in voltage may be due to polarization and/or formation of a thin layer of sodium salt at the electrode/electrolyte interface. The open-circuit voltage (OCV) and short-circuit current (SSC) and other cell profiles for these cells are given in Table 2. Values for the above profiles of a number of cells reported earlier along with data for the present polymer electrolyte cells are given in Table 3.

It is clear that the profiles of cells with the (PVC + $NaIO_4$) electrolyte films are comparable with those reported earlier for various other cells. This suggests a possible application of such cells as solid-state batteries.

4. Conclusions

Optical absorption edge and optical energy gap (both direct and indirect) showed an increasing trend with increased dopant concentration up to 10 wt% of the dopant. The activation energy value obtained from conductivity data decreases with increasing ionic conductivity and vice versa. Using (PVC + $NaIO_4$) polymer electrolyte systems (PESs), electrochemical cells were fabricated and discharge characteristics of these cells were studied. The transference number data indicate that conduction in these electrolytes is predominantly ionic.

Table 2. Various cell parameters for (PVC + $NaIO_4$) polymer electrolytes cells

Cell parameters	Na/(PVC + $NaIO_4$) (X:Y)/(I_2 + C)	
	X:Y = 90:10	X:Y = 80:20
Effective area of the electrolyte/cm^2	2.00	2.00
Cell weight/g	1.50	1.50
Open-circuit voltage (OCV)/V	2.62	2.71
Short-circuit current (SCC)/μA	115	125
Load/kΩ	100	100
Current density/μA cm^{-2}	57.50	62.50
Discharge time for plateau region/h	640	658
Power density/mW kg^{-1}	18.18	21.48
Energy density/mW h kg^{-1}	11635	14133

Table 3. Comparison of present cell profiles with earlier reported data

Solid-state electrochemical cell configuration	Open-circuit voltage (OCV)/V	Short-circuit current (SSC)/μA	Discharge time for plateau region/h	Reference
Na/(PEO + $NaYF_4$)/(I_2 + C + electrolyte)	2.45	560	96	[24]
Na–Hg/(PEO + $NaPF_6$)/(V_2O_5 + C + electrolyte)	2.26	–	–	[25]
Na/(PEO + NaSCN)/(I_2 + C + electrolyte)	2.50	580	100	[26]
Na/(PVC + $NaIO_4$) (90:10)/(I_2 + C)	2.62	115	640	Present
Na/(PVC + $NaIO_4$) (80:20)/(I_2 + C)	2.71	125	658	Present

Acknowledgements

One of the authors (Ch.V.S. Reddy) wishes to thank the Management of Wuhan University of Technology for financial support in the form of a Post Doctoral Fellowship to carry out this work. The Opening Foundation of Hubei Ferroelectric and Piezoelectric Materials and Devices Key Laboratory supported the work. Authors thank Dr. Rajamohan R. Kalluru, Mississippi State University, USA for fruitful discussions.

References

1. M. Onoda, Y. Manada, S. Morita and K. Yoshino, *J. Phys. Soc. Jpn*. **58** (1989) 1895.
2. R. Darbent and T. Olsewska, *Polymer*. **22** (1981) 1655.
3. S. Proneanu, R. Torcu, M. Brie and G. Mihilesan, *Mater. Sci. Forum* **191** (1995) 241.
4. M. Tabata, M. Satoh, K. Kaneto and K. Yoshino, *J. Phys. Soc. Jpn*. **55** (1986) 1305.
5. H. Bhuigan, N.R. Rajapadhya and S.V. Bhoraskar, *Thin Solid Films* **161** (1988) 187.
6. M. Jaipal Reddy, T. Sreekanth and U.V.S. Rao, *Solid State Ionics* **126** (1999) 55–63.
7. P.V. Wright, *Br. Polym. J*. **7** (1975) 319.
8. D.E. Fenton, J.M. Parker and P.V. Wright, *Polymer*. **14** (1973) 589.
9. M.B. Armand, J.M. Chabagno and M. Duclot. *in* P. Vashishta, J.N. Mundy and G.K. Shenoy (eds), Fast Ion Transport in Solids, (North Holland, Amsterdam, 1971).
10. M.B. Armand, J.M. Chabagno and M. Duclot, *Int. Conf. Solid Electrolytes, Ext. Abst* (University of St. Andrews, Scotland, 1988).
11. J.B. Wagner and C. Wagner, *J. Chem. Phys*. **26** (1957) 1597.
12. S.S. Rao, K.V.S. Rao, Md. Shareefuddin, U.V. Subba Rao and S. Chandra, *Solid State Ionics* **67** (1994) 331–335.
13. D.S. Davis and J.S. Shalliday, *Phys. Rev*. **118** (1960) 1020.
14. G.M. Thutupalli and S.G. Tomlin, *J. Phys. D Appl. Phys*. **9** (1976) 1639.
15. A.K. Sharma and Ch. Ramu, *J. Mater. Sci. Lett*. **10** (1991) 1217.
16. K. Yoshino, Y. Manada, K. Sawada, S. Morita, H. Takahashi, R. Sugimoto and M. Onoda, *J. Phys. Soc. Jpn*. **58** (1989) 1320.
17. Ch. Ramu, Y.R.V. Naidu and A.K. Sharma, *Ferroelectrics* **159** (1994) 275.
18. C. Umadevi, A.K. Sharma and V.V.R.N. Rao, *Mater. Lett*. **56** (2002) 167–174.
19. V. Raja, A.K. Sharma and V.V.R.N. Rao, *Mater. Lett*. **57** (2003) 4678–4683.
20. A. Mansingh and S. Kumar, *Thin Solid Films* **161** (1988) 101–106.
21. M.S. Michael, M.M.E. Jacob, S.R.S. Prabaharan and S. Radha Krishna, *Solid State Ionics* **98** (1997) 167–174.
22. S.S. Sekhon, K.V. Pradeep and S.A. Agnihotry. *in* B.V.R. Chowdari, K. Lal, S.A. Agnihotry, N. Khare, S.S. Sekhon, P.C. Srivastava and S. Chandra (eds), Solid State Ionics: Science and Technology, (World Scientific, Singapore, 1998), pp. 217–221.
23. J.L. Souquet, M. Levy and M. Duclot, *Solid State Ionics* **70/71** (1994) 337–345.
24. S.S. Rao, M.J. Reddy, E.L. Narasaiah and U.V. Subba Rao, *Mater. Sci. Eng. B* **33** (1995) 173.
25. S.A. Hashmi, A. Chandra, S. Chandra. *in* B.V.R. Chowdari (ed.), *et al*.Solid State Ionics: Materials and Applications, (World Scientific, Singapore, 1992), pp. 567.
26. H. Yuankang, C. Zhusheng, Z. Zhiyi. *in* B.V.R. Chowdari (ed.), *et al*.Materials for Solid State Ionics, (World Scientific, Singapore, 1986), pp. 333.